

Article

Co-Polymers based on Poly(1,4-butylene 2,5-furandicarboxylate) and Poly(propylene oxide) with Tuneable Thermal Properties: Synthesis and Characterization

Marina Matos ¹, Andreia F. Sousa ^{1,*}, Patrícia V. Mendonça ² and Armando J. D. Silvestre ¹

¹ CICECO and Department of Chemistry, University of Aveiro, 3810-193 Aveiro, Portugal; marina.matos@ua.pt (M.M.); armsil@ua.pt (A.J.D.S.)

² CEMMPRE, Department of Chemical Engineering, University of Coimbra, Rua Sílvio Lima, Pólo II, 3030-790 Coimbra, Portugal; patmend@gmail.com

* Correspondence: andreiafs@ua.pt; Tel.: +351-234-401-470

Received: 11 December 2018; Accepted: 15 January 2019; Published: 21 January 2019



Abstract: Poly(ether ester)s (PEEs) represent a promising class of segmented co-polymers, nevertheless the synthesis of PEEs based on renewable 2,5-furandicarboxylic acid (FDCA) is still scarce. In this context, a series of poly(1,4-butylene 2,5-furandicarboxylate)-*co*-poly(poly(propylene oxide) 2,5-furandicarboxylate) co-polyesters with different composition of stiff poly(1,4-butylene 2,5-furandicarboxylate) (PBF) and soft poly(poly(propylene oxide) 2,5-furandicarboxylate) (PPOF) moieties were synthesized, via a two-step bulk polytransesterification reaction. The molar ratio of PBF/PPOF incorporated was varied (10 to 50 mol%) in order to prepare several novel materials with tuned properties. The materials were characterised in detail through several techniques, namely ATR FTIR, ¹H and ¹³C NMR, TGA, DSC, DMTA and XRD. Their hydrolytic and enzymatic degradation evaluation was also assessed. These new co-polymers showed either a semi-crystalline nature when higher PBF/PPOF ratios were used, and for approximately equal amounts of PBF and PPOF an amorphous co-polyester was obtained instead.

Keywords: 2,5-Furandicarboxylic acid; poly(propylene oxide); poly(ester-ether) co-polymers; tuneable thermal properties

1. Introduction

The massive consumption of fossil-based polymers used on a variety of commodity objects of daily life has prompted, in the last decades, the development of renewable-based alternatives with emphasis on their sustainability. Among the renewable-based polymers, polyesters derived from 2,5-furandicarboxylic acid (FDCA) are some of the most promising. FDCA is a renewable-based aromatic building block monomer that has been widely explored as precursor of several homopolyesters, with very similar properties to those of their non-renewable counterparts, namely terephthalic acid-derivatives (TPA) [1,2].

Some examples of polyesters synthesized from FDCA are poly(ethylene 2,5-furandicarboxylate) (PEF) [3] and poly(1,4-butylene 2,5-furandicarboxylate) (PBF), among others, with similar properties to those of their TPA counterparts [4–11] or even enhanced properties such as for example barrier properties or degradability under enzymatic conditions [12,13]. Furthermore, several other diols besides linear ones have been explored to prepare FDCA-based homopolymers, namely branched diols such as 1,2-propanediol, 2,3-butanediol, 2-methyl-1,3-propanediol and 2,2-dimethyl-1,3-

propanediol [14–20]. The ensuing materials presented even higher T_g s than those of their corresponding homopolyesters synthesized with linear diols with the same number of carbon atoms.

In addition, a demand for new polyesters with specific properties emerged due to the necessity to fulfil specific application gaps, namely in the fields of biomaterials or elastomeric compounds. In this context, some studies [11,21–24] have been focused on the synthesis of FDCA-based poly(ester-ether)s (PEE's) co-polymers composed of polyether soft moieties, for example, poly(butylene glycol) (PBG) [24] and/or poly(ethylene glycol) (PEG) [22,23] to replace their fossil-based counterparts, such as poly(butylene 1,4-terephthalate)-*co*-poly(poly(butylene glycol) 1,4-terephthalate) (PBT-*co*-PBGT) or poly(butylene 1,4-terephthalate)-*co*-poly(poly(ethylene glycol) 1,4-terephthalate) (PBT-*co*-PEGT). Commercial PEEs based on TPA, find important applications among the biomedical field [25,26]. Indeed, PBT-*co*-PEGT co-polymers are commercial PEEs (under trade mark of PolyActive®) [27], and are widely used for drug delivery systems, presenting high thermal stability, as well as enhanced flexibility when compared to PET. This class of polymers show great potential, especially if prepared from FDCA, nonetheless, the literature in furanic PEEs is still scarce [11,21–24]. Zhou et al. [21] presented the first study, reporting the synthesis of poly(1,4-butylene 2,5-furandicarboxylate)-*co*-poly(poly(butylene glycol) 2,5-furandicarboxylate) (PBF-*co*-PBGF) co-polyesters, with enhanced thermal (maximum decomposition temperatures varying from 363 to 378 °C) and mechanical properties (elongation at break between 381 to 832%). Sousa et al. [11] also reported the synthesis of new poly(ester-ether)s co-polymers from FDCA and PEG with different molecular weights (M_n of ~ 200, 400 and 2000), and isosorbide, possessing high thermal stability. More recently, a series of poly(1,4-butylene 2,5-furandicarboxylate)-*co*-poly(poly(ethylene glycol) 2,5-furandicarboxylate) (PBF-*co*-PEGF) co-polyesters were also reported, displaying high thermal stability (up to 380 °C) and low T_g s (ranging from –43.1 to –35.4 °C), enabling their manufacturing process [22,23]. Hydrolytic degradability of PBF-*b*-PEGF was also studied, showing that they can be easily hydrolyzed under alkaline conditions (in phosphate buffered saline (PBS) solution at pH = 12) [23]. Further, Chi et al. [24] also synthesized several PEE's from FDCA, neopentyl glycol and poly(butylene glycol), with enhanced flexibility (elongation at break values from 38 to 1281%).

However, to our knowledge, the use of poly(propylene oxide) (PPO) as co-monomer for the synthesis of PPE co-polymers has not been reported in the literature before. In this context, co-polymerization of FDCA, 1,4-butanediol (BD) and PPO, could be an elegant way to obtain materials with low T_g , facilitating its processability and, at same time, maintaining the thermal stability, thus enlarging the role of potential applications. Precisely, in this study, a series of poly(1,4-butylene 2,5-furandicarboxylate)-*co*-poly(poly(propylene oxide) 2,5-furandicarboxylate) (PBF-*co*-PPOF) co-polyesters were synthesized for the first time by a typical two-step bulk polytransesterification procedure. The ensuing co-polyesters were extensively characterized by SEC, ATR FTIR, ^1H and ^{13}C NMR, TGA, DSC, and DMTA analyses. Importantly, PBF-*co*-PPOF bearing 20 mol% of PPOF moieties was also submitted to a hydrolytic and enzymatic degradability evaluation.

2. Materials and Methods

2.1. Materials

1,4-Butanediol (BD, 99%), poly(propylene oxide) (PPO, average M_n ~1000), deuterated chloroform (CDCl_3 -*d*, 99 atom% D), titanium(IV) tert-butoxide ($\text{Ti}(\text{OBu})_4$, 97%), poly(methyl methacrylate) standards with molecular weights between 4250 and 273,000 sodium phosphate dibasic ($\geq 99\%$), sodium phosphate monobasic ($\geq 99\%$) and Porcine pancreas lipase (Type II, 100-500 units/mg protein) were purchased from Sigma-Aldrich Chemicals Co. 2,5-Furandicarboxylic acid (FDCA, >98%) was purchased from TCI Europe NV. Concentrated hydrochloric acid (37%) was purchased from Panreac; and methanol and chloroform (pro-analysis and HPLC grade) were purchased from Fisher Scientific. All chemicals were used as received, without further purification.

2.2. Synthesis of Dimethyl 2,5-Furandicarboxylate Monomer

The synthesis of DMFDC followed a previously reported procedure [3]. Typically, DMFDC was prepared by reacting FDCA with an excess of methanol, under acidic conditions (HCl), at 80 °C for 15 h. The final product was isolated in 71% yield as a white powder. FTIR (ν/cm^{-1}): 3168 (=C–H); 2965 (C–H); 1706 (C=O); 1578, 1522 (C=C); 1288 (C–O); 1024 (furan ring breathing); 969, 825, 757 (2,5-dibstituted furan ring). ^1H NMR (300 MHz, CDCl_3 , δ / ppm): 7.2 (s, H3/H4 furan ring); 3.9 (s, 2,5-COOCH₃). ^{13}C NMR (75 MHz, CDCl_3 , δ / ppm): 158 (2,5-C=O); 147 (C2/C5 furan ring); 118 (C3/C4 furan ring); 52 (2,5-COOCH₃).

2.3. Syntheses of Poly(1,4-Butylene 2,5-Furandicarboxylate)-Co-Poly(Poly(Propylene Oxide) Co-Polymers and Poly(1,4-Butylene 2,5-Furandicarboxylate)

The polyesters were prepared by a two-step bulk polytransesterification approach following an adapted procedure reported elsewhere [11]. Reactions were carried out by mixing DMFDC (ca. 0.56 g, 3.04 mmol) and a slight excess amount of BD and PPO (ca. 3.22 mmol) (BD/PPO molar ratios of 100/0, 90/10, 80/20, 50/50, Table 1), in the presence $\text{Ti}(\text{O}i\text{Bu})_4$ as catalyst (1 wt% relative to the total mass of monomers). In the first step, the mixture was heated progressively from 100 up to 190 °C, for 5 h, under a nitrogen atmosphere and with constant stirring. In the second step, the reaction proceeded under vacuum (10^{-3} bar) and the temperature was slowly raised to 200 °C for 1h, and finally kept at 210 °C, for 2 h. The ensuing solid products were purified by dissolving in chloroform (~20 mL), and then pouring in an excess of cold methanol, filtered, dried and weighted. In the case of PBF-co-PPOF 50/50 co-polyester (BD/PPO = 50/50), viscous liquid at room temperature, a liquid-liquid extraction procedure using chloroform (~20 mL) was used instead.

Hereafter, the co-polyesters will be referred to as PBF-co-PPOF 90/10, 80/20 and 50/50, according to the BD/PPO molar ratio used as feed. Table 1 presents the molar amounts of each monomer used as well as the weight average molecular weights (M_w) and dispersity ($D = M_w/M_n$) of the polymers.

2.4. Characterization Methods

Size-exclusion chromatography (SEC) analyses of co-polyesters were performed on a Viscotek (Viscotek TDAmx) (Malvern, Gondomar, Portugal) equipped with a differential viscometer (DV) and right-angle laser-light scattering (RALLS, Viscotek) and refractive index (RI) detectors. The column set consisted of a PLgel 5 μm guard column followed by two columns, namely Viscotek T5000 and T4000 column, respectively. A dual piston pump was set with a flow rate of 1 mL min^{-1} . The eluent (DMF with 0.03% LiBr) was previously filtered through a 0.2 μm filter. The system was also equipped with an on-line degasser. The analyses were performed at 60 °C using an Elder CH-150 heater. Before injection, the samples were filtered through a PTFE membrane with 0.2 μm pore. The system was calibrated with narrow poly(methyl methacrylate) standards and the molecular weight and dispersity of the polymers were determined by conventional calibration.

Attenuated total reflectance Fourier transform infrared (ATR FTIR) spectra were obtained using a PARAGON 1000 FTIR spectrometer equipped with a single-horizontal Golden Gate ATR cell (Perkin-Elmer, MA, United States). The spectra were recorded after 128 scans, at a resolution of 4 cm^{-1} , within the range of 500 to 4000 cm^{-1} .

^1H , ^{13}C nuclear magnetic resonance (NMR) spectra were recorded in CDCl_3 using a Bruker AMX 300 spectrometer (Bruker, Madrid, Spain), operating at 300 or 75 MHz, respectively. All chemical shifts (δ) are expressed as parts per million (ppm), downfield from tetramethylsilane (used as the internal standard). Further, the calculation of the real incorporation of BD/PPO ratio ($\text{PBF/PPOF}_{\text{real}}$) the integration areas of OCH_2 proton resonance of F-BD diad ($\delta \approx 4.40$ ppm) and of F-PPO diad ($\delta \approx 3.93$ ppm) were used, according to the equation: $[\text{A}_{\text{OCH}_2\text{F-BD}}/(\text{A}_{\text{OCH}_2\text{F-BD}} + \text{A}_{\text{OCH}_2\text{F-PPO}})]/[\text{A}_{\text{OCH}_2\text{F-PPO}}/(\text{A}_{\text{OCH}_2\text{F-PPO}} + \text{A}_{\text{OCH}_2\text{F-DB}})]$

The Average PBF sequence length was also calculated by the equation: $L_{n,\text{BF}} = 1/[(1 - (\text{PBF}_{\text{real}}/100))] [28]$.

Thermogravimetric analyses (TGA) were carried out with a Setaram SETSYS analyzer (Setaram, Caluire, France) equipped with an alumina plate. Thermograms were recorded under a nitrogen flow of 20 mL min^{-1} and heated at a constant rate of $10 \text{ }^\circ\text{C min}^{-1}$ from room temperature up to $800 \text{ }^\circ\text{C}$. Thermal decomposition temperatures were taken at 5% weight loss step and at maximum decomposition temperatures from the heated samples ($T_{d,5\%}$ and $T_{d,max}$, respectively).

Differential scanning calorimetry (DSC) thermograms were obtained with a Hitachi DSC7000X calorimeter (Hitachi, Paris, France) equipped with a liquid nitrogen cooling system, using aluminum DSC pans. Scans were carried out under nitrogen with a heating rate of $5 \text{ }^\circ\text{C min}^{-1}$ in the temperature range from -90 to $200 \text{ }^\circ\text{C}$. Two heating/cooling cycles were repeated. Glass transition temperature (T_g) was determined using the midpoint approach (second heating trace); and cold crystallization (T_{cc}) and melting (T_m) temperatures were determined as the maximum of the exothermic crystallization peak and the minimum of the melting endothermic peak during the second heating scan, respectively.

Dynamic mechanical thermal analyses (DMTA) were performed using a material pocket accessory with a Triton 2000 DMA (Triton, WA, United States), operating in the single cantilever mode. Tests were performed at 1 and 10 Hz and the temperature was varied from -100 to $200 \text{ }^\circ\text{C}$, at $2 \text{ }^\circ\text{C min}^{-1}$. T_g was determined as the maximum peak of $\tan \delta$.

X-ray diffraction (XRD) measurements were performed using a Philips X'pert MPD diffractometer operating with $\text{CuK}\alpha$ radiation ($\lambda = 1.5405980 \text{ \AA}$) (Malvern, Gondomar, Portugal) at 40 kV and 50 mA. Samples were scanned in the 2θ range of 5 to 50° , with a step size of 0.04° , and time per step of 50 s.

In vitro hydrolytic and enzymatic degradation tests were carried out using press-molded square-shape samples (ca. 69–113 mg) of the prepared polyesters and placed into closed containers with phosphate buffer saline solution (PBS) (10 mL) or with a PBS solution (10 mL) containing Porcine pancreas lipase (concentration of 0.1 mg mL^{-1}), for each test, respectively. The specimens were taken out of the related solution at regular intervals (each 7 days), rinsed thoroughly with distilled water, dried at room temperature for 4 h and weighed. To prevent saturation, both solutions were renewed every 7 days. Each measurement was repeated five times. The weight loss percentage was calculated using the expression: $\text{Weight loss (\%)} = [(W_0 - W_d)/W_0] \times 100$, where, W_0 and W_d stand for the specimens' weights prior and after incubation, respectively.

3. Results and Discussion

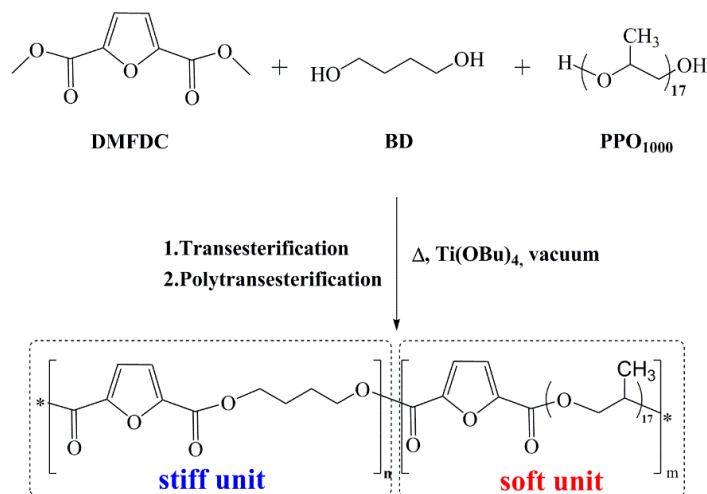
3.1. PBF-co-PPOF Co-Polyesters Synthesis and Structural Characterization

In this study the newly prepared poly(ester-ether) co-polymers are based on poly(1,4-butylene 2,5-furandicarboxylate) as rigid unit and on a soft segment derived from poly(propylene oxide) (Scheme 1). Interestingly, the poly(ether) selected has a methyl side group which plays an important role on the structure-properties features, as discussed ahead.

PBF-co-PPOF were synthesized via a two-step conventional melt polytransesterification approach (Scheme 1) [3], in the presence of $\text{Ti}(\text{O}i\text{Bu})_4$ catalyst and at relatively moderate temperatures, not exceeding $210 \text{ }^\circ\text{C}$, to avoid undesirable side reactions involving the furan moiety (e.g., decarboxylation reactions which are commonly associated to color problem issues) [1]. The resulting polymers were isolated as powders (PBF, PBF-co-PPOF-90/10 and 80/20) or a viscous liquid (PBF-co-PPOF-50/50), in relatively good yields ranging from 65 to 71% (Table 1) in similarity to other FDCA-based polyesters [22]. Furthermore, these co-polyesters showed weight-average molecular weight (M_w) values between 36,700–48,500, and dispersity (D) around 2.

Typical ATR FTIR spectra of all PBF-co-PPOF co-polyesters and related PBF homopolyester (Figure 1) displayed two weak bands near 3150 and 3115 cm^{-1} attributed to the ν C-H bond of the furanic ring. In addition, near 2968 , 2930 , 2893 and 2868 cm^{-1} there are four weak bands attributed to the anti-symmetrical and symmetrical stretching modes (ν C-H *asym* and ν C-H *sym*, respectively) of the C-H bond of methylene and methyl groups related to the BD and PPO moieties, respectively. Additionally, both PBF and co-polyesters spectra exhibited a very intense band near 1725 cm^{-1} , arising

from the C–O stretching vibration, typical of ester groups. Two bands at 1506 and 1573 cm^{-1} , arising from the C–C bond of the furan ring, and C–O–C stretching vibrations appeared at around 1271 cm^{-1} and the typical vibration modes of 2,5-disubstituted furans were observed at 966 , 822 , and 769 cm^{-1} in the case of PBF and PBF-*co*-PPOF materials. The presence of the abovementioned bands confirmed the success of the polymerization reactions.



Scheme 1. Synthesis of PBF-*co*-PPOF co-polymers.

Table 1. Molecular characteristics of PBF and PBF-*co*-PPOF *co*-polymers.

(co)polymer	BD/PPO _{feed} ¹ (mol%)	Yield (%) ²	M_w ³	\bar{D} ⁴
PBF	100/0	71.0	-	- ⁵
PBF- <i>co</i> -PPOF-90/10	90/10	64.8	36 700	2.2
PBF- <i>co</i> -PPOF-80/20	80/20	68.1	41 600	2.2
PBF- <i>co</i> -PPOF-50/50	50/50	71.4	48 500	2.1

¹ Molar feed percentage of BD and PPO units. ² Isolation yields of purified polyesters in methanol. ³ Weight-average molecular weight. ⁴ Dispersity. ⁵ Not determinate due to the insolubility of PBF in DMF.

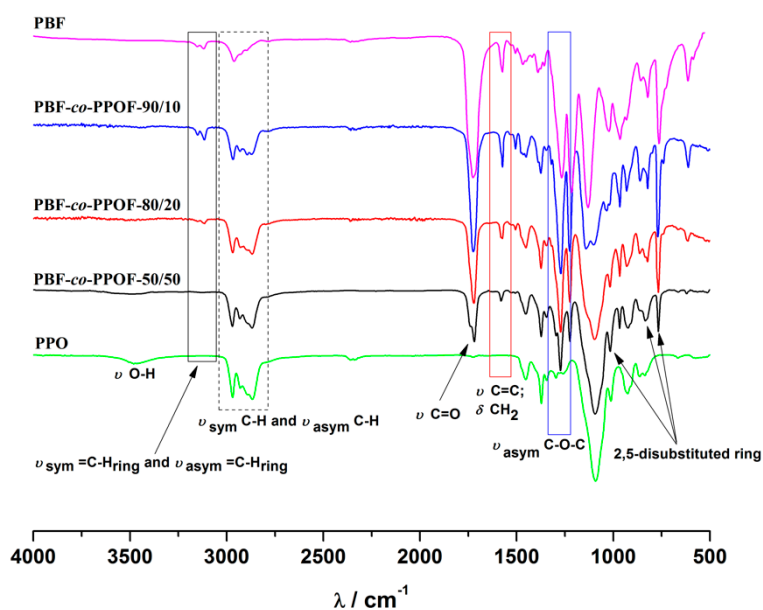


Figure 1. ATR FTIR spectra of PBF-*co*-PPOF co-polymers.

The chemical structure characterization of all PBF-co-PPOF co-polyesters and PBF homopolyester was also studied by ^1H (Figure 2 and Table 2), ^{13}C NMR (Table 4 and Figure S1) and 2D analysis (Figure S2). The main ^1H NMR resonances and respective assignments of all polymers studied are summarized in Table 2 and Figure 2 displays the ^1H NMR spectrum of PBF-co-PPOF-90/10.

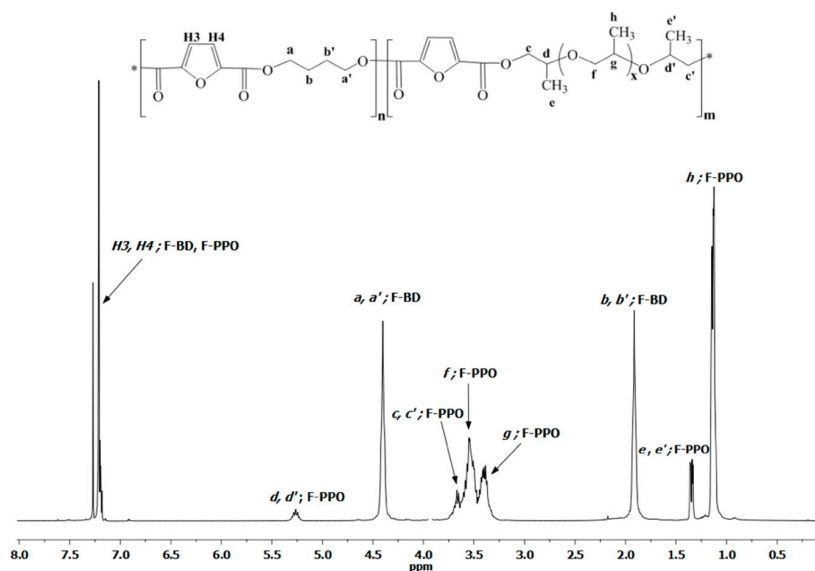


Figure 2. ^1H NMR spectrum of PBF-co-PPOF-90/10 co-polymer in $\text{CHCl}_3\text{-}d$.

Table 2. Main ^1H NMR resonances of PBF-co-PPOF co-polyesters, and PBF and PPO homopolyesters. The a, b, c, d, e, f, g and a', b', c', d', e' attributions are explained in the scheme of Figure 2.

δ/ppm	Assignment	Diads	Integration Area				
			PBF	PBF-co-PPOF		PPO	
				90/10	80/20		50/50
7.21	H3 and H4; CH	F-BD; FDCA-PPO	1.00	1.00	1.00	1.00	
5.26	d, d'; CHCH_3	F-PPO	–	0.14	0.37	0.92	
4.40	a, a'; $\text{C}(\text{O})\text{OCH}_2\text{CH}_2$	F-BD	2.01	1.66	1.28	0.46	
3.67	c, c'; $\text{C}(\text{O})\text{OCH}_2$	F-PPO	–	0.30	0.84	1.84	
3.54	f; OCH_2	PPO-PPO	–	1.91	5.14	17.89	2.01
3.40	g; OCH	PPO-PPO	–	1.03	2.77	9.46	1.00
1.91	b, b'; $\text{C}(\text{O})\text{OCH}_2\text{CH}_2$	F-BD	2.01	1.66	1.41	0.48	
1.34	e, e'; CHCH_3	F-PPO	–	0.44	1.30	3.04	
1.15	h; OCHCH_3	PPO-PPO	–	3.10	8.60	28.50	3.02

The ^1H NMR spectra of all polymers (Figure 2 and Table 2) displayed the typical resonances attributed to the F-BD diad at approximately δ 7.21, 4.40 and 1.91 attributed to the H3 and H4 protons of the furan ring, and to the $\text{C}(\text{O})\text{OCH}_2\text{CH}_2$ and $\text{C}(\text{O})\text{OCH}_2\text{CH}_2$ protons of the BD moiety, respectively. In the co-polymers spectra, the corresponding resonances associated to the PPO-F diads were also detected: δ 5.26, 3.67 and 1.34 ppm, arising from the $\text{C}(\text{O})\text{OCH}$, $\text{C}(\text{O})\text{OCH}_2$ and $\text{C}(\text{O})\text{OCHCH}_3$ protons, in the neighboring of the furan ring, respectively. Moreover, the protons related to the PPO-PPO units were also identified at δ 3.54, 3.40, and 1.15 ppm, related to OCH_2 (ether linkage), OCH and OCHCH_3 , respectively.

Furthermore, the ^1H NMR spectra data was used to access the real molar percentage of PBF and PPOF moieties in the co-polyesters backbone, due to the important impact this ratio has on the ensuing co-polyesters properties. The PBF/PPOF real incorporation was determined using the integration areas of $\text{C}(\text{O})\text{OCH}_2$ proton resonances (in the neighboring of furan ring) of the F-BD (δ at 4.40 ppm) and F-PPO (δ at 3.93 ppm) diads, respectively, and the main results are presented in Table 3.

Table 3. Comparison between the initial and the real molar ratio percentages of PBF and PPOF in the polyesters' backbone.

(co)polymer	PBF/PPOF _{feed} ¹	PBF/PPOF _{real} ²	$L_{n,BF}$ ³
PBF	100/0	100/0	–
PBF-co-PPOF-90/10	90/10	85/15	6.5
PBF-co-PPOF-80/20	80/20	76/24	4.2
PBF-co-PPPOF-50/50	50/50	20/80	1.3

¹ Molar feed ratio percentage of BD and PPO units. ² Molar real ratio percentage of BD and PPO units. ³ Average PBF sequence length.

From Table 3, it is possible to observe that despite the BD and PPO feed ratio, there was a tendency for a higher incorporation of PPOF into co-polyesters chains, most probably associated with BD lost during the polytransesterification step due to the high BD volatility. However, this trend is almost negligible in the case of the PBF-co-PPOF-90/10 and 80/20 co-polyesters.

The number average sequence length of BF unit ($L_{n,BF}$) was also assessed assuming that PBF-co-PPOF co-polyesters are random co-polyesters. It was found that $L_{n,BF}$ increased with the BF content increasing, according with the theoretically expected values [11,22,29,30]. Importantly, the co-polyester with the highest amount of PBF (PBF-co-PPOF-90/10) had a $L_{n,BF}$ of 6.5. This is an important structural feature that is in accordance with a crystalline domain dominated by PBF segments and corresponding melting behavior, as discussed above.

In terms of ¹³C NMR analysis (Table 4 and Figure S1), the observed resonances were in agreement with their expected chemical structure and corroborated the above ¹H NMR results, as well as the ATR FTIR data.

Table 4. Main ¹³C NMR resonances of all PBF-co-PPOF co-polyesters, and PBF and PPO homopolyester. The a, b, c, d, e, f, g and a', b', c', d', e' attributions are explained in the scheme of Figure 2.

Assignment	Diads	Integration Area				
		PBF	PBF-co-PPOF		PPO	
			90/10	80/20		50/50
2-CO and 5-CO; C(O)O	F-BD; F-PPO	158.0	158.0	158.0	158.0	-
C2 and C5; C-C(O)O	F-BD; F-PPO	146.8	146.8	146.8	147.0	-
C3 and C4; C-H	F-BD; F-PPO	118.5	118.5	118.5	118.2	-
f; OCH ₂	PPO-PPO	-	75.4	75.3	75.3	75.3
g; OCH	PPO-PPO	-	73.4	73.4	73.4	74.4
c, c'; C(O)OCH ₂	F-PPO	-	72.9	72.9	72.9	-
d, d'; CHCH ₃	F-PPO	-	71.7	71.7	71.3	-
a, a'; C(O)OCH ₂ CH ₂	F-BD	64.9	64.9	64.9	64.8	-
b, b'; C(O)OCH ₂ CH ₂	F-BD	25.4	25.4	25.3	25.0	-
h; OCHCH ₃	PPO-PPO	-	17.3	17.3	17.3	17.3
e, e'; CHCH ₃	F-PPO	-	16.9	16.8	16.8	-

3.2. X-Ray Diffraction Analysis

The XRD patterns of PBF-co-PPOF-90/10 and 80/20 co-polymers (Figure 3) indicated that they were semi-crystalline polymers, displaying both an amorphous halo around $2\theta \sim 21^\circ$ and diffraction peaks at $2\theta \approx 18, 23$ and 25° , quite similar to the PBF pattern although in the former case peaks were more intense than for the co-polymers probably due to a higher crystallinity. In fact, the PBF XRD pattern (Figure 3), exhibited intense diffraction peaks at $2\theta \sim 10, 18, 23$ and 25° [16,31–33]. This clearly indicates that the ability of PBF-co-PPOF co-polyesters to crystallize is mainly associated to PBF segments (with $L_{n,BF}$ equal to 6.5 and 4.2, respectively). Moreover, these results are in perfect agreement with the below DSC and DMTA data, and also with other FDCA or TPA-based PPEs reported in the literature [21,22,34,35].

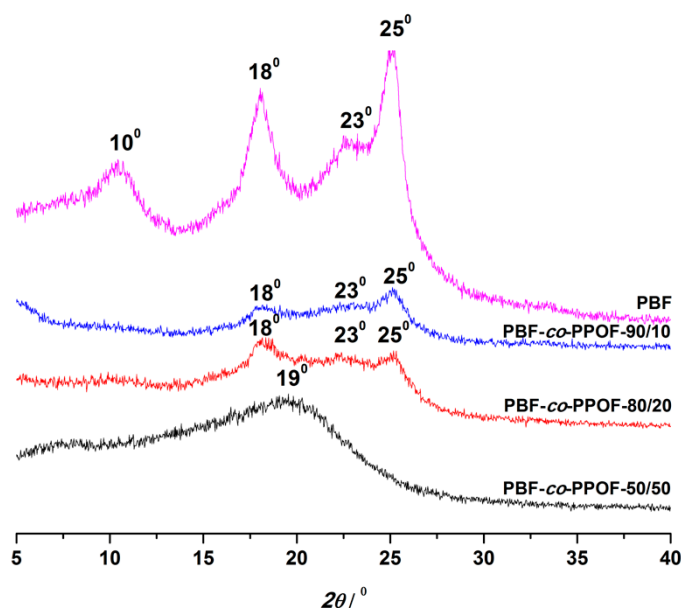


Figure 3. XRD patterns of PBF and all PBF-co-PPOF materials.

As expected, in the case of the viscous liquid PBF-co-PPOF-50/50 co-polyester, only a halo centered at $2\theta \approx 19^\circ$ was observed, in accordance with an essential amorphous nature.

3.3. Thermal Behaviour

PBF-co-PBDG co-polyesters were extensively characterized in terms of their thermal behavior through DSC, DMTA and TGA analyses (Table 5, and Figures S3–S6).

Table 5. Decomposition at 5% weight loss ($T_{d,5\%}$), maximum decomposition ($T_{d,max}$), glass transition (T_g) and melting temperature (T_m) of PBF, PPO and PBF-co-PPOF co-polyesters.

co(polymer)	DSC ¹		DMTA ²		TGA ³	
	$T_m/^\circ\text{C}$	$T_g/^\circ\text{C}$	$T_m/^\circ\text{C}$	$T_{d,5\%}/^\circ\text{C}$	$T_{d,max}/^\circ\text{C}$	
PBF	170.0	75.6	166.9	348.7	380.5	
PBF-co-PPOF-90/10	137.7	−32.6	147.6	284.7	347.2	
PBF-co-PPOF-80/20	124.1	−37.2	124.2	288.9	340.3	
PBF-co-PPOF-50/50	-	−42.3	- ³	308.1	365.2	
PPO		−67.0–72.0 ⁵	-	283.0	323.4	

¹ Determined by DSC analysis. ² Determined by DMTA analysis. ³ Determined by TGA analysis. ⁴ Values obtained from references [36,37].

The semi-crystalline character of the co-polymers having higher PBF/PPOF molar ratios (PBF-co-PPOF-90/10 and 80/20) was confirmed by DSC and DMTA analyses (Figures S3–S5). For example, the DSC trace of PBF-co-PPOF-90/10 co-polyester (Figure S4) displayed glass transition (T_g) and melting temperatures (T_m) at -49.7 and 137.7°C , respectively. The PBF-co-PPOF-80/20 co-polyester also maintained some ability to crystallize and melt, with a cold transition (T_{cc}) and T_m of approximately 21.7 and 124.1°C (Table 5), similar to the one of PBF (T_m of 170.0°C). Furthermore, using DMTA analysis (Figure S5), T_g values of -32.6 , -37.2 and -42.3°C for PBF-co-PPOF-90/10, 80/20 and 50/50 materials were observed, respectively; and T_m of 147.6 and 124.2°C for PBF-co-PPOF-90/10 and 80/20 were detected. In the case of PBF-co-PPOF-50/50 co-polymer (having a lower PBF/PPOF molar ratio) the absence of T_m is in accordance with its essential amorphous nature (XRD data).

In summary, the highly desirable properties obtained included, the T_g of the co-polyesters decreased with the increasing content of soft PPOF segments (tailored behavior), although these results

were still higher than those of amorphous PPO homopolymer (T_g between -67 to -72 °C [36,37]). These results were expected since the incorporation of more PPO flexible moieties into FDCA-based co-polyesters typically gives rise to a decrease on the co-polymers' thermal features [21,22]. Importantly, the co-polymers with higher BF content, PBF-co-PPOF-90/10 and 80/20, showed a typical segmented polymers behavior [22], with a T_m very close to that of stiff PBF and a T_g below room temperature closer to that of soft PPO, revealing that PBF units were the main responsible for the crystalline behavior of the ensuing materials, whereas the PPOF segments were associated with the amorphous domain. Hence, for PBF-co-PPOF-90/10 the range of working temperatures was quite enlarged: within -39 and 139 °C.

In general the TGA thermograms (Table 5 and Figure S6) of the co-polyesters (carried out under nitrogen atmosphere) exhibited one major characteristic event at the maximum decomposition temperatures ($T_{d,max}$) of 340 – 365 °C. Also, the newly prepared co-polymers showed to be thermally stable up to $T_{d,5\%} \approx 308$ °C.

As shown in Table 5, the co-polymers had both $T_{d,5\%}$ and $T_{d,max}$ results lower than those observed to PBF. These less favorable thermal results could be associated with the presence of the appending methyl group, as already reported for other polyesters also having side groups, such as poly(2,3-butylene 2,5-furandicarboxylate) compared to PBF [17]. Nevertheless, all PBF-co-PPOF co-polyesters have higher $T_{d,max}$ than PPO.

3.4. Hydrolytic and Enzymatic Degradation Tests

As mentioned above, in addition to specific thermal properties, it was also important to understand if the newly prepared materials degraded under hydrolytic and enzymatic conditions for a relatively short period of time. The evaluation of the hydrolytic and enzymatic degradation behavior was performed in terms of weight loss percentage versus time (Figure 4) for PBF-co-PPOF-80/20 co-polyester, with real incorporation of PPOF moieties around 24 mol%. However, the polymer's weight loss under hydrolytic conditions was almost negligible for a relatively short period of 12 weeks, and a little bit higher under enzymatic conditions (2.3%). This result was in the same line with those reported for PBF-co-PEGF co-polyesters incorporating similar amount of PBF moieties [23], and also with studies on PBT-co-PEGT co-polyesters in similar hydrolytic conditions as the ones used in this study (pH ~ 7 and 37 °C) [38].

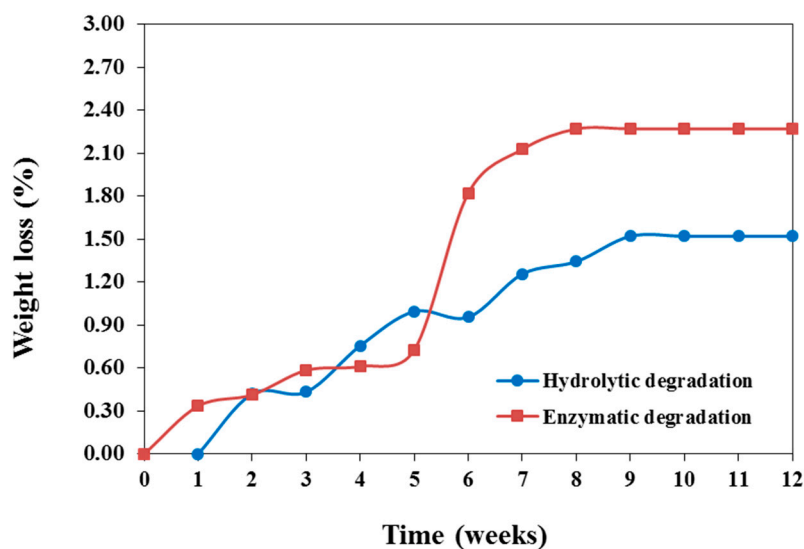


Figure 4. Weight loss percentage of PBF-co-PPOF-80/20 co-polyester along 12 weeks.

The incubation with a Porcine pancreas lipase in PBS solution slightly increased the weight loss of the co-polyester, but it was still very low. Through hydrolytic and enzymatic degradation only 1.5 and

2.3% weight loss were achieved, respectively. Nevertheless, the data obtained are good preliminary results, and showed some evidence of degradation of PBF-co-PPOF (also checked by FTIR) associated with the hydrolysis of the ester groups, but further studies using other enzymes such as for example cutinases, could enhance the results obtained. Some positive results were previously obtained with cutinase from *Humicola insolens* or *Thermobifida cellulositytica* to hydrolyze PET and PEF [12,13]. Further, incorporation of PPO in the co-polymers, is also, expected to enhance degradability.

4. Conclusions

In conclusion, a new class of FDCA-based poly(ester-ether) co-polymers has been accomplished, incorporating both stiff and soft moieties into their backbone. The ensuing co-polyesters have shown high thermal stability ($T_{d,max}$ between 340 to 365 °C) and T_g at sub-ambient temperatures, namely from −42.3 to −32.6 °C. Moreover, the semi-crystalline character was only observed for co-polyesters with higher BF content, revealing that PBF units were mainly responsible for the crystalline behavior of the ensuing materials, whereas the PPOF were associated with the amorphous domain. Furthermore, PBF-co-PPOF-80/20 co-polyester had shown a week hydrolysable behavior, presenting a maximum percentage weight loss of 2.3 %, after 12 weeks.

Finally, due to their high thermal stability, as well as the presence of both stiff and soft moieties in the co-polymer chains, these materials could find interesting industrial applications, namely as thermoplastic polymers.

Supplementary Materials: The following are available online at <http://www.mdpi.com/1996-1944/12/2/328/s1>, Figure S1: ^{13}C NMR spectra in $\text{CHCl}_3\text{-d}$ of PBF-co-PPOF-90/10 copolymer, Figure S2: 2D NMR spectrum in $\text{CHCl}_3\text{-d}$ of PBF-co-PPOF-90/10 copolymer, Figure S3: DSC curve of PBF homopolymer. Figure S4: DSC curves (second scan) of all PBF-co-PPOF copolymers studied, Figure S5: $\tan \delta$ of PBF and PBF-co-PPOF (co)polymers, at 1 Hz, Figure S6: TGA (a) and DTGA (b) thermograms of PBF-co-PPOF copolymers and PBF homopolymer.

Author Contributions: Supervision, A.J.D.S. and A.F.S.; conceptualization, A.F.S.; investigation, M.M.; SEC analysis performance, P.V.M.

Acknowledgments: FCT and POPH/FSE are gratefully acknowledged for funding a doctoral grant to MM (PD/BD/52501/2014) and the post-doctoral grant of PVM (SFRH/BPD/117589/2016). The costs resulting from the FCT hiring of AFS was funded by national funds (OE), through FCT – Fundação para a Ciência e a Tecnologia, I.P., in the scope of the framework contract foreseen in the numbers 4, 5 and 6 of the article 23, of the Decree-Law 57/2016, of August 29, changed by Law 57/2017, of July 19. This work was developed within the scope of the project CICECO-Aveiro Institute of Materials, FCT Ref. UID/CTM/50011/2019, financed by national funds through the FCT/MCTES.

Conflicts of Interest: The authors declare no conflicts of interest.

References

1. De Jong, E.; Dam, M.A.; Sipos, L.; Gruter, G.-J. Furan dicarboxylic acid (FDCA), a versatile building block for a very interesting class of polyesters. In *Biobased Monomers, Polymers, and Materials*; Smith, P.B., Gross, R.A., Eds.; ACS Symposium Series; American Chemical Society: Washington, DC, USA, 2012; Volume 1105, pp. 1–13, ISBN 0-8412-2767-5.
2. Jia, Z.; Wang, J.; Sun, L.; Zhu, J.; Liu, X. Fully bio-based polyesters derived from 2,5-furandicarboxylic acid (2,5-FDCA) and dodecanedioic acid (DDCA): From semicrystalline thermoplastic to amorphous elastomer. *J. Appl. Polym. Sci.* **2018**, *135*, 46076. [[CrossRef](#)]
3. Gandini, A.; Silvestre, A.J.D.; Neto, C.P.; Sousa, A.F.; Gomes, M. The furan counterpart of poly(ethylene terephthalate): An alternative material based on renewable resources. *J. Polym. Sci. Polym. Chem.* **2009**, *47*, 295–298. [[CrossRef](#)]
4. Sousa, A.F.A.F.; Vilela, C.; Fonseca, A.C.; Matos, M.; Freire, C.S.R.; Gruter, G.-J.M.; Coelho, J.F.J.; Silvestre, A.J.D. Biobased polyesters and other polymers from 2,5-furandicarboxylic acid: A tribute to furan excellency. *Polym. Chem.* **2015**, *6*, 5961–5983. [[CrossRef](#)]
5. Zhang, D.; Dumont, M.J. Advances in polymer precursors and bio-based polymers synthesized from 5-hydroxymethylfurfural. *J. Polym. Sci. Part A Polym. Chem.* **2017**, *55*, 1478–1492. [[CrossRef](#)]

6. Papageorgiou, G.Z.; Papageorgiou, D.G.; Terzopoulou, Z.; Bikiaris, D.N. Production of bio-based 2,5-furan dicarboxylate polyesters: Recent progress and critical aspects in their synthesis and thermal properties. *Eur. Polym. J.* **2016**, *83*, 202–229. [[CrossRef](#)]
7. Gomes, M.; Gandini, A.; Silvestre, A.J.D.; Reis, B. Synthesis and characterization of poly(2,5-furan dicarboxylate)s based on a variety of diols. *J. Polym. Sci. Polym. Chem.* **2011**, *49*, 3759–3768. [[CrossRef](#)]
8. Sousa, A.F.; Matos, M.; Freire, C.S.R.; Silvestre, A.J.D.; Coelho, J.F.J. New copolyesters derived from terephthalic and 2,5-furandicarboxylic acids: A step forward in the development of biobased polyesters. *Polymer* **2013**, *54*, 513–519. [[CrossRef](#)]
9. Matos, M.; Sousa, A.F.; Silvestre, A.J.D. Improving the thermal properties of poly(2,5-furandicarboxylate)s using cyclohexylene moieties: A comparative study. *Macromol. Chem. Phys.* **2017**, *218*, 1600492. [[CrossRef](#)]
10. Soares, M.J.; Dannecker, P.-K.; Vilela, C.; Bastos, J.; Meier, M.A.R.; Sousa, A.F. Poly(1,20-eicosanediyl 2,5-furandicarboxylate), a biodegradable polyester from renewable resources. *Eur. Polym. J.* **2017**, *90*, 301–311. [[CrossRef](#)]
11. Sousa, A.F.; Coelho, J.F.J.; Silvestre, A.J.D. Renewable-based poly((ether)ester)s from 2,5-furandicarboxylic acid. *Polymer* **2016**, *98*, 129–135. [[CrossRef](#)]
12. Weinberger, S.; Canadell, J.; Quartinello, F.; Yenzi, B.; Arias, A.; Pellis, A.; Guebitz, G. Enzymatic degradation of poly(ethylene 2,5-furanoate) powders and amorphous films. *Catalysts* **2017**, *7*, 318. [[CrossRef](#)]
13. Weinberger, S.; Haernvall, K.; Scaini, D.; Ghazaryan, G.; Zumstein, M.T.; Sander, M.; Pellis, A.; Guebitz, G.M. Enzymatic surface hydrolysis of poly(ethylene furanoate) thin films of various crystallinities. *Green Chem.* **2017**, *19*, 5381–5384. [[CrossRef](#)]
14. Haernvall, K.; Zitzenbacher, S.; Amer, H.; Zumstein, M.T.; Sander, M.; McNeill, K.; Yamamoto, M.; Schick, M.B.; Ribitsch, D.; Guebitz, G.M. Polyol structure influences enzymatic hydrolysis of bio-based 2,5-furandicarboxylic acid (FDCA) polyesters. *Biotechnol. J.* **2017**, *12*, 1600741. [[CrossRef](#)] [[PubMed](#)]
15. Gubbels, E.; Jasinska-Walc, L.; Koning, C.E. Synthesis and characterization of novel renewable polyesters based on 2,5-furandicarboxylic acid and 2,3-butanediol. *J. Polym. Sci. Polym. Chem.* **2013**, *51*, 890–898. [[CrossRef](#)]
16. Thiyagarajan, S.; Vogelzang, W.; Knoop, R.J.; Frissen, A.E.; van Haveren, J.; van Es, D.S. Biobased furandicarboxylic acids (FDCAs): Effects of isomeric substitution on polyester synthesis and properties. *Green Chem.* **2014**, *16*, 1957. [[CrossRef](#)]
17. Jiang, Y.; Woortman, A.J.J.; van Ekenstein, G.O.R.A.; Loos, K. A biocatalytic approach towards sustainable furanic-aliphatic polyesters. *Polym. Chem.* **2015**, *6*, 5198–5211. [[CrossRef](#)]
18. Terzopoulou, Z.; Kasmi, N.; Tsanaktis, V.; Doullakas, N.; Bikiaris, D.N.; Achilias, D.S.; Papageorgiou, G.Z. Synthesis and characterization of bio-based polyesters: Poly(2-methyl-1,3-propylene-2,5-furanoate), Poly(isosorbide-2,5-furanoate), Poly(1,4-cyclohexanedimethylene-2,5-furanoate). *Materials* **2017**, *10*, 801. [[CrossRef](#)]
19. Tsanaktis, V.; Terzopoulou, Z.; Exarhopoulos, S.; Bikiaris, D.N.; Achilias, D.S.; Papageorgiou, D.G.; Papageorgiou, G.Z. Sustainable, eco-friendly polyesters synthesized from renewable resources: Preparation and thermal characteristics of poly(dimethyl-propylene furanoate). *Polym. Chem.* **2015**, *6*, 8284–8296. [[CrossRef](#)]
20. Genovese, L.; Lotti, N.; Siracusa, V.; Munari, A. Poly(neopentyl glycol furanoate): A member of the furan-based polyester family with smart barrier performances for sustainable food packaging applications. *Materials* **2017**, *10*, 1028. [[CrossRef](#)]
21. Zhou, W.; Zhang, Y.; Xu, Y.; Wang, P.; Gao, L.; Zhang, W.; Ji, J. Synthesis and characterization of bio-based poly(butylene furandicarboxylate)-b-poly(tetramethylene glycol) copolymers. *Polym. Degrad. Stab.* **2014**, *109*, 21–26. [[CrossRef](#)]
22. Sousa, A.F.; Guigo, N.; Pozycka, M.; Delgado, M.; Soares, J.; Mendonça, P.V.; Coelho, J.F.J.; Sbirrazzuoli, N.; Silvestre, A.J.D. Tailored design of renewable copolymers based on poly(1,4-butylene 2,5-furandicarboxylate) and poly(ethylene glycol) with refined thermal properties. *Polym. Chem.* **2018**, *9*, 722–731. [[CrossRef](#)]
23. Hu, H.; Zhang, R.; Sousa, A.; Long, Y.Y.; Ying, W.B.; Wang, J.; Zhu, J. Bio-based poly(butylene 2,5-furandicarboxylate)-b-poly(ethylene glycol) copolymers with adjustable degradation rate and mechanical properties: Synthesis and characterization. *Eur Polym J* **2018**, *106*, 42–52. [[CrossRef](#)]

24. Chi, D.; Liu, F.; Na, H.; Chen, J.; Hao, C.; Zhu, J. Poly(neopentyl glycol 2,5-furandicarboxylate): A Promising Hard Segment for the Development of Bio-based Thermoplastic Poly(ether-ester) Elastomer with High Performance. *ACS Sustain. Chem. Eng.* **2018**, *6*, 9893–9902. [[CrossRef](#)]
25. Deschamps, A.A.; Claese, M.B.; Sleijster, W.J.; Bruijn, J.D.; Grijpma, D.W.; Feijen, J. Design of segmented poly(ether ester) materials and structures. *J. Control. Release* **2002**, *78*, 175–186. [[CrossRef](#)]
26. Buitinga, M.; Truckenmüller, R.; Engelse, M.A.; Moroni, L.; Ten Hoopen, H.W.; van Blitterswijk, C.A.; de Koning, E.J.; van Apeldoorn, A.A.; Karperien, M. Microwell Scaffolds for the Extrahepatic Transplantation of Islets of Langerhans. *PLoS ONE* **2013**, *8*, 1–11. [[CrossRef](#)] [[PubMed](#)]
27. Octoplus PolyActive™ A Biodegradable Polymer-Based Drug Delivery System. Available online: <http://www.octoplus.nl/nl/Contact/News> (accessed on 3 December 2018).
28. Deschamps, A.A.; Grijpma, D.W.; Feijen, J. Poly(ethylene oxide)/poly(butylene terephthalate) segmented block copolymers: The effect of copolymer composition on physical properties and degradation behavior. *Polymer* **2001**, *42*, 9335–9345. [[CrossRef](#)]
29. Wang, J.; Liu, X.; Jia, Z.; Liu, Y.; Sun, L.; Zhu, J. Synthesis of bio-based poly(ethylene 2,5-furandicarboxylate) copolyesters: Higher glass transition temperature, better transparency, and good barrier properties. *J. Polym. Sci. Part A Polym. Chem.* **2017**, *55*, 3298–3307. [[CrossRef](#)]
30. Wang, J.; Liu, X.; Zhu, J.; Jiang, Y. Copolyesters based on 2,5-furandicarboxylic acid (FDCA): Effect of 2,2,4,4-tetramethyl-1,3-cyclobutanediol units on their properties. *Polymers* **2017**, *9*, 305. [[CrossRef](#)]
31. Gandini, A.; Coelho, D.; Gomes, M.; Reis, B.; Silvestre, A. Materials from renewable resources based on furan monomers and furan chemistry: Work in progress. *J. Mater. Chem.* **2009**, *19*, 8656. [[CrossRef](#)]
32. Jiang, M.; Liu, Q.; Zhang, Q.; Ye, C.; Zhou, G. A series of furan-aromatic polyesters synthesized via direct esterification method based on renewable resources. *J. Polym. Sci. Polym. Chem.* **2012**, *50*, 1026–1036. [[CrossRef](#)]
33. Ma, J.; Yu, X.; Xu, J.; Pang, Y. Synthesis and crystallinity of poly(butylene 2,5-furandicarboxylate). *Polymer* **2012**, *53*, 4145–4151. [[CrossRef](#)]
34. Yao, C.; Yang, G. Crystallization, and morphology of poly(trimethylene terephthalate)/poly(ethylene oxide terephthalate) segmented block copolymers. *Polymer* **2010**, *51*, 1516–1523. [[CrossRef](#)]
35. Szymczyk, A. Structure and properties of new polyester elastomers composed of poly(trimethylene terephthalate) and poly(ethylene oxide). *Eur. Polym. J.* **2009**, *45*, 2653–2664. [[CrossRef](#)]
36. Allen, G.; Crossley, H.G. Polypropylene oxide IV-Preparation and properties of polyether networks. *Polymer* **1964**, *5*, 553–557. [[CrossRef](#)]
37. Vesterinen, A.; Lipponen, S.; Rich, J.; Seppälä, J. Effect of block composition on thermal properties and melt viscosity of poly[2-(dimethylamino)ethyl methacrylate], poly(ethylene oxide) and poly(propylene oxide) block co-polymers. *Express Polym. Lett.* **2011**, *5*, 754–765. [[CrossRef](#)]
38. Chao, G.T.; Fan, L.Y.; Jia, W.J.; Qian, Z.Y.; Gu, Y.C.; Liu, C.B.; Ni, X.P.; Li, J.; Deng, H.X.; Gong, C.Y.; et al. Synthesis, characterization and hydrolytic degradation of degradable poly(butylene terephthalate)/poly(ethylene glycol) (PBT/PEG) copolymers. *J. Mater. Sci. Mater. Med.* **2007**, *18*, 449–455. [[CrossRef](#)]



© 2019 by the authors. Licensee MDPI, Basel, Switzerland. This article is an open access article distributed under the terms and conditions of the Creative Commons Attribution (CC BY) license (<http://creativecommons.org/licenses/by/4.0/>).